Porous Media Project

Ahmad

July 6, 2020

Contents

1 Introduction

In order to study the porous media, we introduce a model that captures flow behavior through a porous material. We consider the porous media as a network of pores that are connected together through connections. The schematic of our model is shown in Fig. 1. We use a random resistor networks on a structured grid as our model to study the flow behavior. Each node represents a pore and each edge represents the throats between pores. We use simple Poiseuille flow through pipes to model fluid flow through pipes. In each pipe with diameter d, length L, and pressure difference of ΔP on both sides, results in a flow Q, where

$$\frac{\Delta P}{L} = \frac{128}{\pi} \frac{\mu Q}{d^4} \tag{1}$$

where μ is the viscosity of the fluid. The above relation is known as Darcy's law.
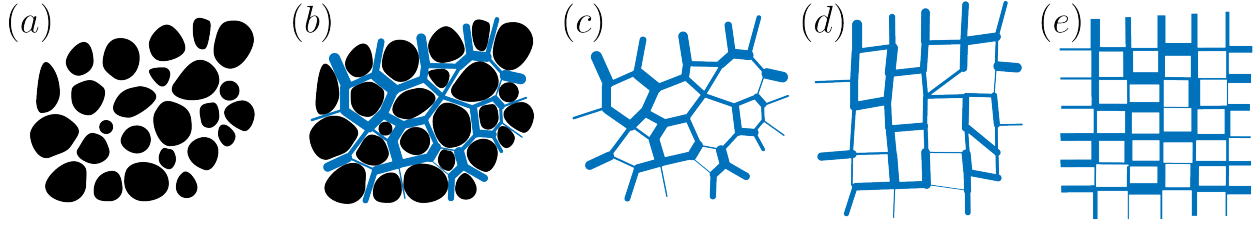
Figure 1: Schematic of the network model for porous media: (a) a sample cross section of a porous media. (b) The porous media can be considered as a network of pores connected through resistive connections. (c) The random network obtained from porous media. (d) Reordering the porous media network on a structured grid. (e) The ordered structured network used where the connections are assumed to be random resistors.

2 Numerical Simulation

We consider a network of tubes with a random distribution of diameters as shown in Fig. porous-schematice. Darcy's law is obtained thought the momentum equation and relates the pressure and the flow through the pipes. Furthermore, at each node the summation of the inflows should add up to zero (conservation of mass). Using this a system of equations $AP = B$ is obtained where P is the vector of pressures at nodes, A is sparse where the nonzero elements are

$$A_{ii} = \sum_{j \text{ neighbors of } i} \frac{\pi}{128\mu L} d_{ij}^4 \tag{2}$$

$$A_{ij} = \begin{cases} -\frac{\pi}{128\mu L} d_{ij}^4, & \text{if } j \text{ is neighbor of } i \\ 0, & \text{otherwise} \end{cases} \tag{3}$$

Note that if all the pipes have the same diameter, then the flow is only in the horizontal pipes, and vertical pipes will carry no flow.

Numerical results

We consider a 2d network of pipes, and a pressure difference between the left and right nodes. We further assume different distribution of pipe diameters and find the flow q in the pipes. When the pipes are all the same diameter, then the velocities in the pipes are either 0 or some nonzero value. As we increase the randomness in the pipes, we observe that the PDF of velocities starts to follow an exponential tail trend. Interestingly, if the disorder in pipes diameter is large enough, the PDF of velocities in the pipes, no matter what distribution we pick follows the same distribution.

3 Analytical results

In order to describe the universality observed above, we introduce the following mode. First, instead of using the structured rectangular grid, we use a structured diagonal grid. This will
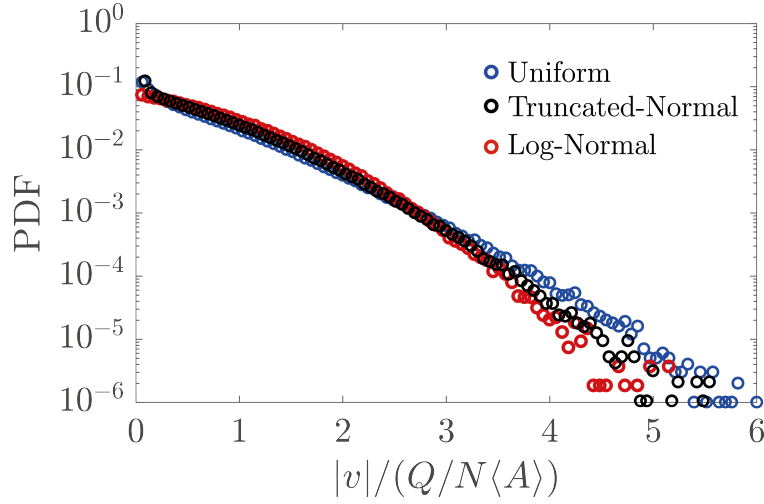
Figure 2: PDF of normalized velocities of the pipes in a random network of pipes, v is the velocity in the pipe, Q is the total flux, N is the number of pipes in the vertical direction, $\langle A \rangle$ is the average of the area of the pipe. Note that $N\langle A \rangle$ is the average area carrying the flow Q.
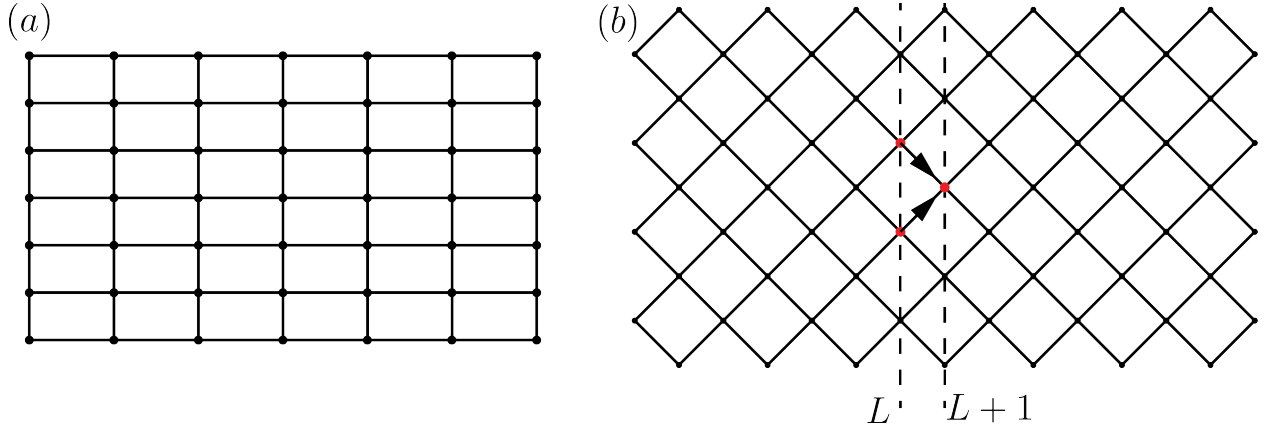
simplify the analytical model (see Fig. 3).

Figure 3: Schematic of grids: (a) The structured rectangular grid used in the numerical simulation. (b) The structured diagonal grid used in the analytical model.

We assume that the total flow to node i at level L is noted by $Q(L, i)$. This flow is then redistributed to the neighboring nodes at the level $L+1$. We assume that this redistribution is done by weights w_{ij} as

$$Q(L+1, j) = \sum_i w_{ij} Q(L, i) = w_{i,i+1} Q(L, i+1) + w_{i,i} Q(L, i) \tag{4}$$

where $\sum_j w_{ij} = 1$ (since the total outflow from node i is $\sum_j q_i w_{ij}$ and this value should add up to q_i). We assume that w_{ij} are drawn from a distribution $\eta(w)$. Since $\eta(w)$ is a

distribution, then $\int \eta(w)dw = 1$. Furthermore, since $\sum_j w_{ij} = 1$, we can conclude that

$$\sum_j w_{ij} = 1 \rightarrow NE[w_{ij}] = 1 \rightarrow E[w_{ij}] = 1/N \rightarrow \int w\eta(w)dw = 1/N \tag{5}$$

Now we use the technique of mean field analysis for a general distribution of $\eta(w)$ to find the distribution of Q at the layers. The values of $Q(D,i)$ are not independent for neighboring sites; however, the mean field approximation ignores these correlations. We have

$$P_L(Q) = \prod_{j=1}^{N} \left\{ \int_0^1 dw_j \eta(w_j) \int_0^\infty dQ_j P_{L-1}(Q_j) \right\} \times \delta \left(\sum_j w_j Q_j - Q \right) \tag{6}$$

The constraint that Q's emanating downward should add up to one is in the definition of $\eta(w)$. The only approximation in the above equation is that we neglect the possible correlation between the values of Q among ancestors. If we take the Laplace transform of the above equation, we obtain

$$\tilde{P}(s) \equiv \int_0^\infty P(Q)e^{-Qs}dQ \tag{7}$$

$$\xrightarrow{\int_0^\infty (\cdot)e^{-Qs}dQ} P(Q) = \prod_{j=1}^{N} \left\{ \int_0^1 dw_j \eta(w_j) \int_0^\infty dQ_j P(Q_j) \right\} \times \delta \left(\sum_j w_j Q_j - Q \right) \tag{8}$$

$$\tilde{P}(s) = \int_0^\infty \prod_{j=1}^{N} \left\{ \int_0^1 dw_j \eta(w_j) \int_0^\infty dQ_j P(Q_j) \right\} \times \delta \left(\sum_j w_j Q_j - Q \right) e^{-Qs}dQ \tag{9}$$

$$= \prod_{j=1}^{N} \left\{ \int_0^1 dw_j \eta(w_j) \int_0^\infty dQ_j e^{-\sum w_j Q_j} P(Q_j) \right\} \tag{10}$$

$$= \prod_{j=1}^{N} \left\{ \int_0^1 dw_j \eta(w_j) \tilde{P}(sw_j) \right\} \tag{11}$$

$$= \left(\int_0^1 dw \eta(w) \tilde{P}(sw) \right)^N \tag{12}$$

Or to summarize

$$\boxed{\tilde{P}(s) = \left(\int_0^1 dw \eta(w) \tilde{P}(sw) \right)^N} \tag{13}$$

Note that in the above equation N determines the number of neighboring sites and in our structured diamond grid $N = 2$. The above equation is recursively converges to a distribution. If we set $\eta(w) = \delta(w - 1/2)$, then the flow at each node has probability of $1/2$ to move up or down. As a result the flow at a given depth L will be homogeneous as $P_L(Q) = \delta(Q - \bar{Q})$ where $\bar{Q}$ is the average of input fluid flow. This case is the same as the same diameter which results in a singular solution in the structured grid.

4

$P(Q)$ decays faster than Q^{-n} for any n

We first show that $P(Q)$ decays faster than any power of Q for any weight distributions. We expand the Laplace transform as

$$\tilde{P}(s) = 1 + \sum_j \tilde{P}_j s^j \tag{14}$$

Inserting this expansion into Eq. (13), we obtain

$$1 + \sum_j \tilde{P}_j s^j = \left(\int_0^1 dw \eta(w) \left[1 + \sum_j \tilde{P}_j (sw)^j \right] \right)^N \tag{15}$$

$$= \left(1 + \sum_j \tilde{P}_j \langle w^j \rangle s^j \right)^N \tag{16}$$

where $\langle w^j \rangle = \int_0^1 \eta(w) w^j dw$ is the j-th moment of the weights w. In the above equation we can observe that

$$P_j \left(N \langle w^j \rangle - 1 \right) = G(P_{j-1}, P_{j-1}, \cdots, P_1) \tag{17}$$

In the above equation P_j can only diverge only if $N\langle w^j \rangle - 1$ is zero. If w can only be zero and one, then $\langle w^j \rangle = \langle w \rangle = 1/N$ and the coefficient can become zero! Other than this special distribution where $0 \leq w \leq 1$, then

$$w \in [0,1] \to w > w^2 > w^3 > \cdots \tag{18}$$

$$\forall k > 1 \to \langle w^k \rangle < \langle w \rangle = \frac{1}{N} \tag{19}$$

which means that $N\langle w^j \rangle - 1$ is not zero and as a result P_j is finite. P_j on the other hand is the j-th moment or $\langle Q^j \rangle$ and it is finite. If $P \approx Q^{-n}$, then the n-th moment will not be finite i.e. $\langle Q^{n+1} \rangle = P_{n+1}$ is not finite. We can then conclude that $P(Q)$ should go to zero faster than any Q^{-n} as $Q \to \infty$! In other words $d \log P(Q)/d \log Q \to -\infty$ as $Q \to \infty$.

Exponential Decay

The main governing equation for a diamond grid is

$$\tilde{P}(s) = \left(\int_0^1 dw \eta(w) \tilde{P}(sw) \right)^2 \tag{20}$$

In order to have an approximation for $\eta(w)$ we do the following: At each node there are two nodes where the flux is distributed by w_1 and w_2. Lets assume that w_1 is uniformly distributed between 0 and 1. As a result $w_2 = 1 - w_1$ (since conservation of mass $w_1 + w_2 = 1$).

Now $\eta(w)$ can be found as

$$\eta(w) = M \int_0^1 dw_1 \delta(1 - w_1 - w) = M, \tag{21}$$

$$\text{since } \int_0^1 \eta(w)dw = 1 \rightarrow M = 1 \tag{22}$$

$$\eta(w) = 1 \tag{23}$$

Just for completeness, if there are three connections ($N = 3$), then we have

$$\eta(w) = M \int_0^1 dw_1 \int_0^1 dw_2 \delta(1 - w_1 - w_2 - w) \tag{24}$$

$$= M(1 - w) \rightarrow \int_0^1 \eta(w)dw = 1 \rightarrow M = \frac{1}{2} \tag{25}$$

$$\eta(w) = \frac{1}{2}(1 - w) \tag{26}$$

As a result the main equation simplifies to

$$\tilde{P}(s) = \left(\int_0^1 dw \tilde{P}(sw) \right)^2 \tag{27}$$

In order to solve the above equation, we assume $\tilde{V}(s) = \sqrt{\tilde{P}(s)}$.

$$\tilde{V}(s) = \int_0^1 dw \tilde{V}(sw) = \int_0^s \frac{du}{s} \tilde{V}^2(u) \tag{28}$$

$$s\tilde{V}(s) = \int_0^s du \tilde{V}^2(u) \tag{29}$$

$$\tag{30}$$

Taking the differentiation with respect to s yields

$$\tilde{V}(s) + s \frac{d\tilde{V}(s)}{ds} = \tilde{V}^2(s) \tag{31}$$

$$\frac{d\tilde{V}}{\tilde{V}^2 - \tilde{V}} = \frac{ds}{s} \tag{32}$$

$$\log\left(\frac{1 - \tilde{V}}{\tilde{V}} \right) = \log(s) \tag{33}$$

$$\tilde{V}(s) = \frac{1}{1 + Cs} \tag{34}$$

6

We set the mean to 1 i.e.,

$$\int_0^\infty QP(Q)dQ = 1 \rightarrow \frac{d\tilde{P}}{ds}\Big|_{s=0} = -1 \tag{35}$$

$$\frac{d\tilde{V}}{ds} = \frac{1}{2\sqrt{\tilde{P}(s)}}\frac{d\tilde{P}(s)}{ds} \rightarrow \frac{d\tilde{V}(s)}{ds}\Big|_{s=0} = \frac{-1}{2} \tag{36}$$

$$\frac{d\tilde{V}(s)}{ds} = \frac{-C}{(1+Cs)^2}\Big|_{s=0} = -C = \frac{-1}{2} \rightarrow C = \frac{1}{2} \tag{37}$$

As a result, we have

$$\tilde{P}(s) = \left(\frac{1}{1+s/2}\right)^2 \tag{38}$$

$$P(Q) = 4Qe^{-2Q} \tag{39}$$

We can then show that for a uniform distribution of w's, the PDF of Q's become an exponential tail. For other distribution of w's, we similarly find a similar trend. Actually, we should that the PDF of Q should decay faster than any power law for any distribution of w. Note that the only parameter that determines the the PDF of the flow is the average flux. This shows that why we observe the universal behaviour for pdf.

4   Continuous Limit

In the previous section (§3), we used a toy model to describe the flow behavior. The main equation connecting the flow at different layers was Eq. (4). In this section, we are interested to see what a continuous limit of the above model will be. Consider Eq. (4) as

$$Q(i, j+1) = w_{i-1,j}Q(i-1, j) + w_{i+1,j}Q(i+1, j) \tag{40}$$

where we had a constraint on the weights as

$$w_{i-1,j} + w_{i+1,j} = 1 \tag{41}$$

Now, lets assume that these weights are perturbations around the a uniform distribution such that

$$w_{i\pm1,j} = \frac{1}{2}(1 \pm v_{i\pm1,j}) \tag{42}$$

with th above assumption, we find that

$$Q(i, j + 1) = \frac{1}{2} \left(1 - v_{i-1,j}\right) Q(i - 1, j) + \frac{1}{2} \left(1 + v_{i+1,j}\right) Q(i + 1, j) \tag{43}$$

$$Q + L_y \frac{\partial Q}{\partial y} + L_y^2 \frac{\partial^2 Q}{\partial y^2} = \frac{1}{2}(1 - v + L_x \frac{\partial v}{\partial x}) \left(Q - L_x \frac{\partial Q}{\partial x} + \frac{1}{2} L_x^2 \frac{\partial Q^2}{\partial x^2}\right)$$

$$+ \frac{1}{2}(1 + v + L_x \frac{\partial v}{\partial x}) \left(Q + L_x \frac{\partial Q}{\partial x} + \frac{1}{2} L_x^2 \frac{\partial^2 Q}{\partial x^2}\right) \tag{44}$$

$$L_y \frac{\partial Q}{\partial y} = L_x v \frac{\partial Q}{\partial x} + L_x \frac{\partial v}{\partial x} Q + \frac{L_x^2}{2} \frac{\partial^2 Q}{\partial x^2} \tag{45}$$

$$\frac{\partial Q}{\partial y} = \frac{L_x}{L_y} \frac{\partial}{\partial x} (vQ) + \frac{L_x^2}{2L_y} \frac{\partial^2 Q}{\partial x^2} \tag{46}$$

Assuming that $L_x = L_y$ (similar length scales in both directions), we find that

$$\boxed{\frac{\partial Q}{\partial y} = \frac{\partial}{\partial x} (vQ) + D \frac{\partial^2 Q}{\partial x^2}} \tag{47}$$

which is a convection-diffusion equation. It seems that y direction (the direction where flow propagates into the porous medium) acts similar to time. As the flow moves inward, the Q diffuses in the x direction, and convects with velocity v.

5   Network Evolution

Any changes to the micro-structure in a porous medium, such as solute retention during polymer flow (effectively" clogging" some pores in the network), affects the pore-level flow and alters the bulk behavior. In this section, we want to study the effect of such evolution in the network. The radius of the pipes in the network, can reduce (due to clogging) or increase (due to erosion). The rate of such reduction (or increase) can depend on flux, or shear rate, or velocity, or etc. We can simplify these models with all the models with the following equation

$$\frac{dR}{dt} \propto \pm \frac{Q}{R^n} \tag{48}$$

where $n = 0, 2, 3$ corresponds to proportionality with flow rate, velocity, shear gradient respectively. The plus sign corresponds to erosion, and the negative sign corresponds to the clogging. In order to study the effect of the above equation in whole network, we first study the effect in a two parallel/series case.

5.1   Erosion

In erosion the rate of change of radius reads as

$$\frac{dr}{dt} = \alpha \frac{Q}{r^n} \tag{49}$$

8

Here, note that each pipe with radius R acts as a resistor, we have Poissoulle flow equation that relates the flow Q to pressure difference ΔP as

$$Q = \frac{-\pi r^4}{8\mu L}\Delta P \tag{50}$$

$$Q = -C(r)\Delta P, \quad C(r) = \frac{\pi r^4}{8\mu L} = \beta r^4 \tag{51}$$

Two pipes in series

We consider two pipes in series as shown in Fig. 4. We are interested to see what happens two the resistors for different initial conditions? How does the values of the resistors evolve? What happens to the pressure distribution at the note in between?
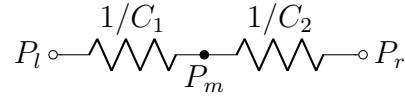
Figure 4: Two resistors at series

We first simulate the results numerically to see what happens. The results are shown in Fig. 5. As it can be seen, for any initial conditions the pressure at the middle point, converges to $(P_l + P_r)/2$ which basically means that the flow is homogenized.

We now show why this convergence happens. If the two pipes are in series, then Q is always the same in these two pipes. Therefore

$$\frac{dr}{dt} = \alpha\frac{Q}{r^n} \tag{52}$$

$$r^n dr = \alpha Q dt \tag{53}$$

$$\frac{1}{n+1}r^{n+1} - \frac{1}{n+1}r_0^{n+1} = \alpha Q t \tag{54}$$

$$r = \left((n+1)\alpha Q t + r_0^{n+1}\right)^{\frac{1}{n+1}} \tag{55}$$

$$C_i = \beta\left((n+1)\alpha Q t + r_{i,0}^{n+1}\right)^{\frac{4}{n+1}} \tag{56}$$

So the pressure at the middle point becomes as

$$Q = \frac{1}{1/C_1 + 1/C_2}\Delta P = \text{const.}, \tag{57}$$

$$P_m - P_l = \frac{Q}{C_1} \tag{58}$$

$$P_r - P_l = \frac{1}{1/C_1 + 1/C_2}Q \tag{59}$$

$$\frac{P_m - P_l}{P_r - P_l} = \frac{1/C_1}{1/C_1 + 1/C_2} = \frac{C_2}{C_1 + C_2} \tag{60}$$
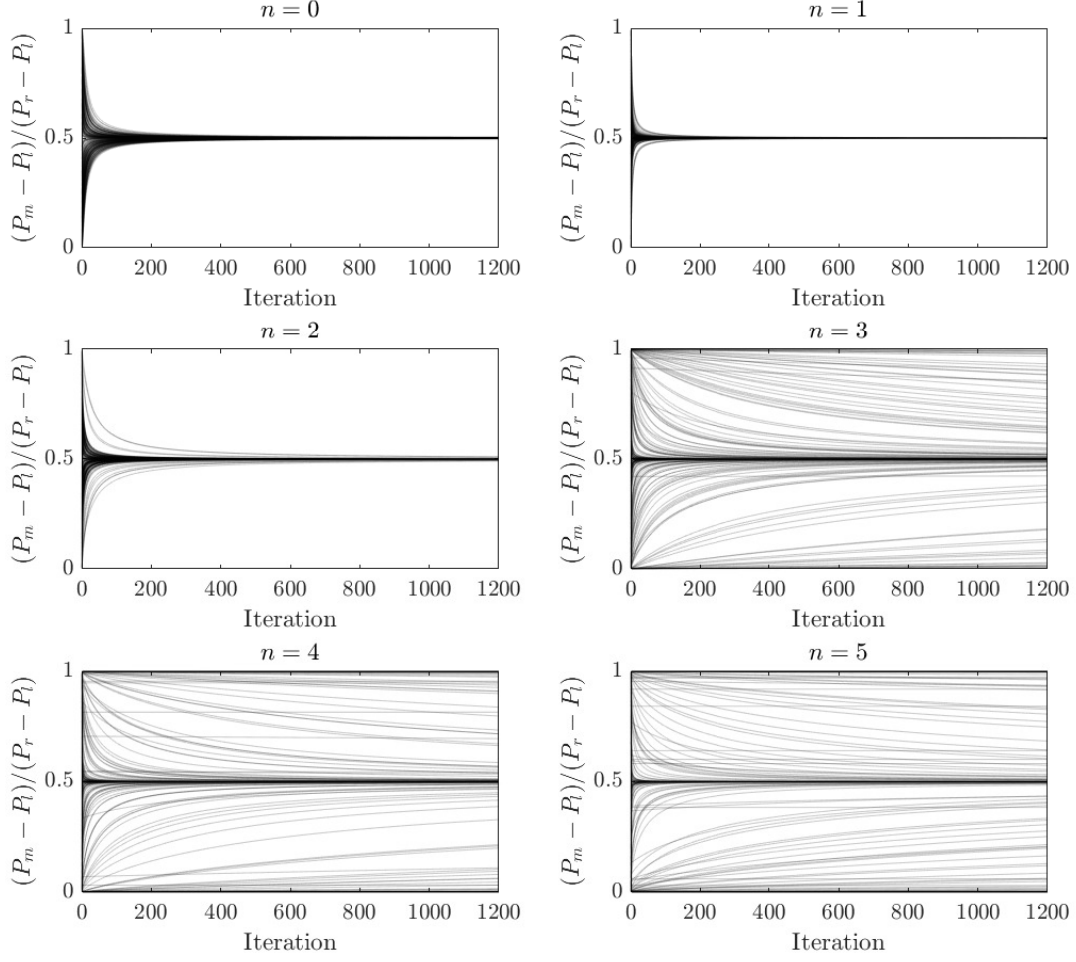
9

Figure 5: Toy model for two pipes in series. In each iteration, we change the radius of the pipe as $r_{\mathrm{new}} = r_{\mathrm{old}} + \alpha Q / r_{\mathrm{old}}^n$. For all different cases of n the middle pressure converges to $(P_l + P_r)/2$.

Combining the results we find that

$$\boxed{\frac{P_m - P_l}{P_r - P_l} = \frac{\beta \left((n+1)\alpha Q t + r_{2,0}^{n+1} \right)^{\frac{4}{n+1}}}{\beta \left((n+1)\alpha Q t + r_{1,0}^{n+1} \right)^{\frac{4}{n+1}} + \beta \left((n+1)\alpha Q t + r_{2,0}^{n+1} \right)^{\frac{4}{n+1}}}} \tag{61}$$

$$\lim_{t \to \infty} \frac{P_m - P_l}{P_r - P_l} = \frac{1}{2} \tag{62}$$

Note that for any power of n the pressure in the middle point as $t \to \infty$ converges to $(P_l + P_r)/2$.

10

Two Parallel Pipes Case

Now assume two pipes in parallel as shown in Fig. 6. We first simulate the results to see what happens for different initial conditions. The results for different initial values of r_1, r_2 are shown in Fig. 7.
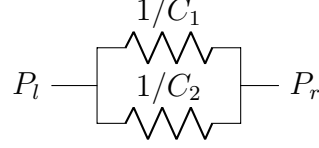

Figure 6: Two resistors parallel together

Now, we start to model to see why this happens. Initially, we note that

$$Q_1 = C_1 \Delta P, \quad \text{and} \quad Q_2 = C_2 \Delta P \tag{63}$$

$$Q = (C_1 + C_2)\Delta P \tag{64}$$

We change the radius of each pipe according to its flow, as a result, we have

$$\frac{dr_1}{dt} = \alpha \frac{Q_1}{r_1^n}, \qquad \frac{dr_2}{dt} = \alpha \frac{Q_2}{r_2^n} \tag{65}$$

$$r_1^n \frac{dr_1}{dt} + r_2^n \frac{dr_2}{dt} = \alpha(Q_1 + Q_2) = \alpha Q \tag{66}$$

On the other hand, we know that

$$\Delta P = \frac{Q_1}{C_1} = \frac{Q_2}{C_2} \tag{67}$$

$$\Delta P = \frac{Q_1}{\beta r_1^4} = \frac{Q_2}{\beta r_2^4} \tag{68}$$

$$\frac{dr_i}{dt} = \alpha \frac{Q_i}{r_i^n} = \frac{\alpha \beta \Delta P}{r_i^{n-4}} \tag{69}$$

We have

$$r_1^{n-4} \frac{dr_1}{dt} = r_2^{n-4} \frac{dr_2}{dt} \tag{70}$$

$$\text{if } n = 3, \quad \rightarrow \log(\frac{r_1}{r_{1,0}}) = \log(\frac{r_2}{r_{2,0}}), \rightarrow r_1 = \gamma r_2 \tag{71}$$

$$\text{if } n \neq 3, \quad r_1^{n-3} - r_2^{n-3} = \gamma \tag{72}$$

where γ is a constant. In the above equation, without loss of generality, we can assume that
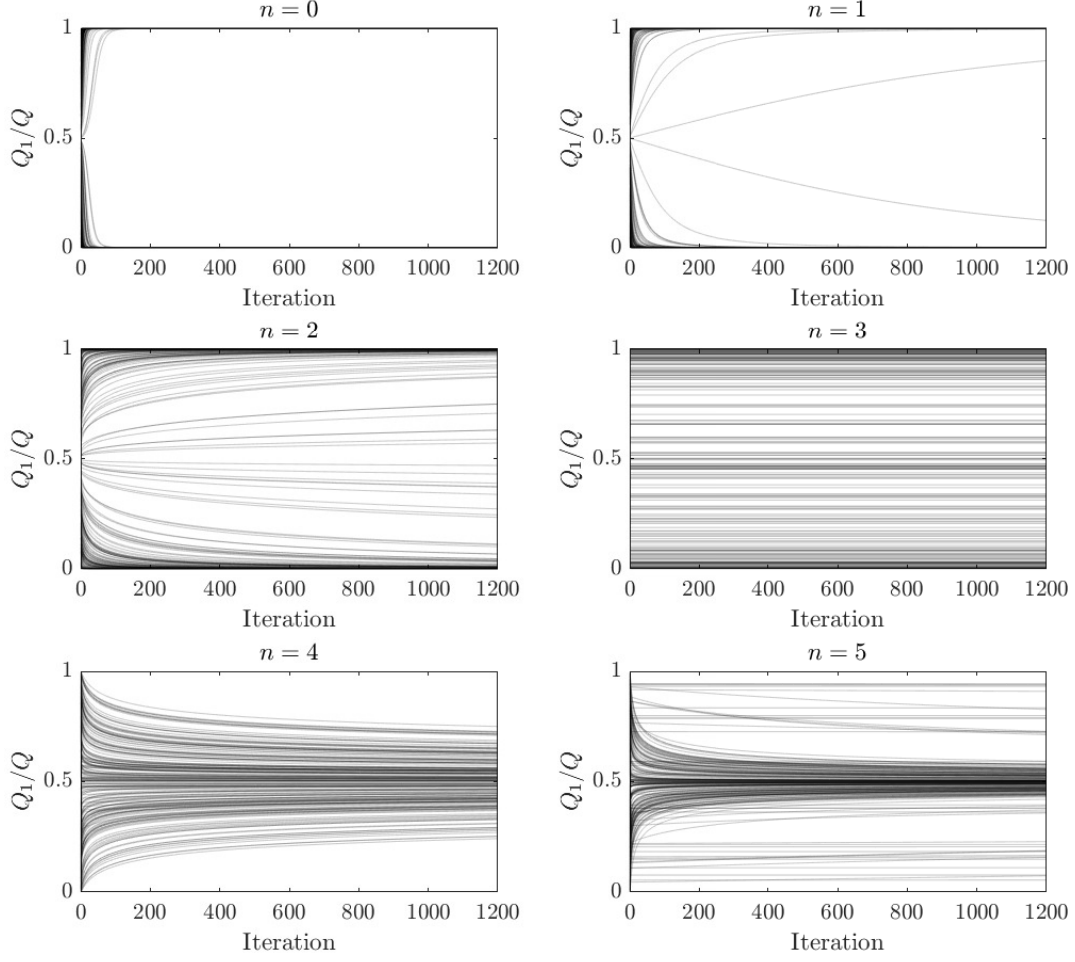
11

Figure 7: Toy model for two pipes in parallel. In each iteration, we change the radius of the pipe as $r_{\text{new}} = r_{\text{old}} + \alpha Q_i / r_{\text{old}}^n$. When $n < 3$, all of the flow eventually passes from either top or bottom pipe. When $n = 3$, the flow proportion remains the same. When $n > 3$, the flow homogenizes where half of the total flow i.e. $Q/2$ passes from top and the other half from bottom pipe.

$r_1 > r_2$ and γ is positive. Now, looking at the other part of the equation, we have

$$\frac{dr_2}{dt} = \alpha \frac{Q_2}{r_2^4} = \frac{\alpha \beta \Delta P}{r_2^{n-4}} \tag{73}$$

$$= \frac{\alpha \beta}{r_2^{n-4}} \frac{Q}{\beta(r_2^4 + r_1^4)} = \frac{\alpha Q}{r_2^n + r_2^{n-4} r_1^4} \tag{74}$$

$$= \frac{\alpha Q}{r_2^n + r_2^{n-4} \left(r_2^{n-3} + \gamma\right)^{\frac{4}{n-3}}} \tag{75}$$

$$\left[r_2^n + r_2^{n-4} \left(r_2^{n-3} + \gamma\right)^{\frac{4}{n-3}} \right] dr_2 = \alpha Q dt \tag{76}$$

$$\frac{1}{n+1} \left[r_2^{n+1} + \left(r_2^{n-3} + \gamma\right)^{\frac{n+1}{n-3}} \right] = \alpha Q t + C \tag{77}$$

$$r_2^{n+1} + \left(r_2^{n-3} + \gamma\right)^{\frac{n+1}{n-3}} = (n+1)\left(\alpha Q t + C\right) \tag{78}$$

$$r_2^{n+1} + r_1^{n+1} = At + B \tag{79}$$

So the two set of equations summarizes to

$$\begin{cases} r_1^{n-3} - r_2^{n-3} = \gamma & \text{if } n \neq 3, \\ r_1 = \gamma r_2 & \text{if } n = 3 \end{cases} \tag{80}$$

$$r_1^{n+1} + r_2^{n+1} = At + B \tag{81}$$

The plot for the solution to the above equations for different values of $n \neq 3$ and also the separate solution for $n = 3$ is shown in the following figure.
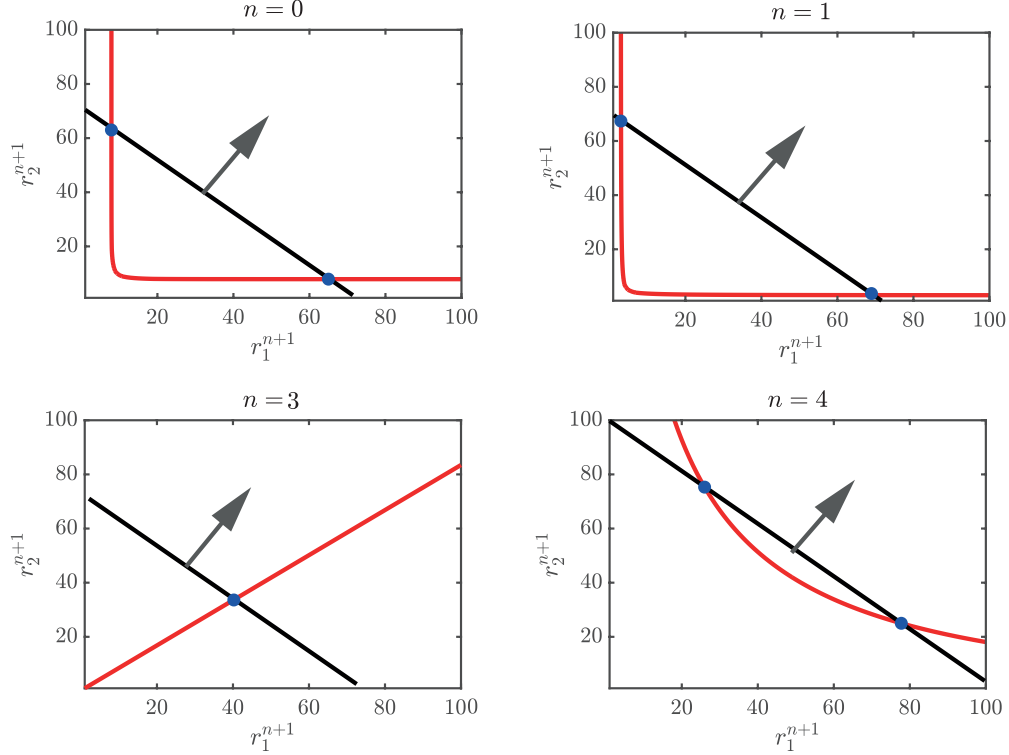

Figure 8: Analytical solution for r_1 and r_2 for parallel resistors. For different n the solution changes. Specifically, if $n < 3$, then one of the diameters stops varying while the other one increases in size. If $n = 3$, the both grow together, and if $n > 3$ then they both increase in size.

General Case

In a general case, the resistors can be divided into series and parallel resistors. Using that in each section, we only need to look at the parallel resistors and determine the channelling. The resistors in series do not affect the channelling to occur. They only contribute tot he homogenization. Parallel resistors however, in the case of $n > 3$ result in channeling. Note that at some places, we might need to use $\Delta - Y$ conversion to find the equivalent resistors. It can be shown that the channeling can still be described using $\Delta - Y$ conversion.

5.2 Clogging

In clogging, the rate of change of radius reads as

$$\frac{dr}{dt} = -\alpha \frac{Q}{r^n} \tag{82}$$

Similar to the erosion, we first study a simplified model with two pipes in series and parallel.

Series

We consider the following pattern for the resistors (Fig. 9). We first simulate for different initial conditions, and look at the middle pressure over long time. Since the radius is decreasing, we need to set a maximum amount of reduction. Since the radius cannot become negative. For different initial conditions we look at the middle pressure, and we observe that no matter what power of n is, the middle pressure remains almost unchanged. If the minimum threshold is hit, then some jumps can be observed, however, the total behavior is such that the ratio of the middle pressure remains almost similar.
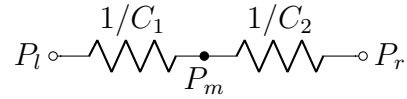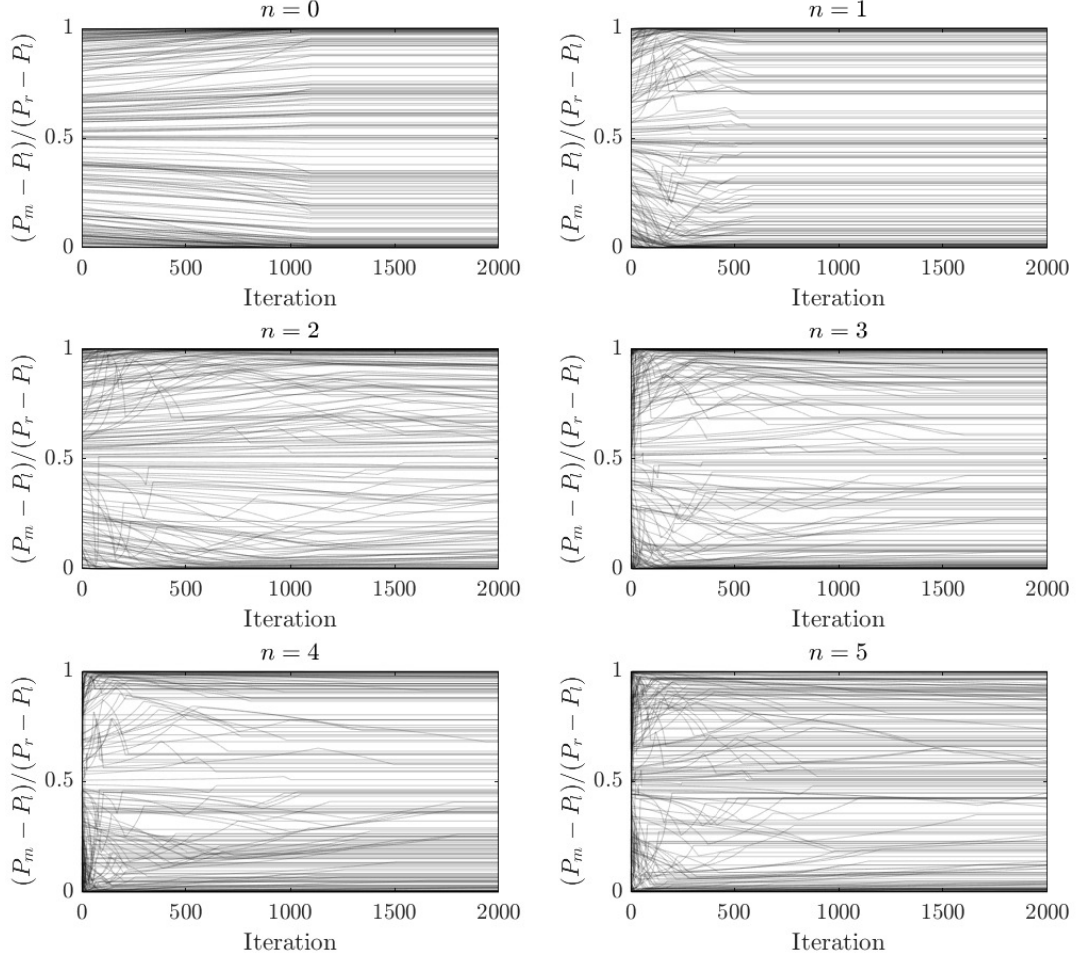

Figure 9: Two resistors at series

Figure 10: Toy model for two pipes in series. In each iteration, we change the radius of the pipe as $r_{\text{new}} = r_{\text{old}} - \alpha Q_i / r_{\text{old}}^n$. Note that we set a maximum change of $\Delta r = \min{1, r}$.

Parallel

We also study the behavior when the pipes are in parallel (See Fig. 11). The numerical results of the simulations are shown in Fig. 12. The behavior is again very similar to the two pipes in series. We again find a similar trend where the ratio of the Q's remains unchanged.
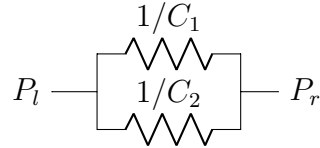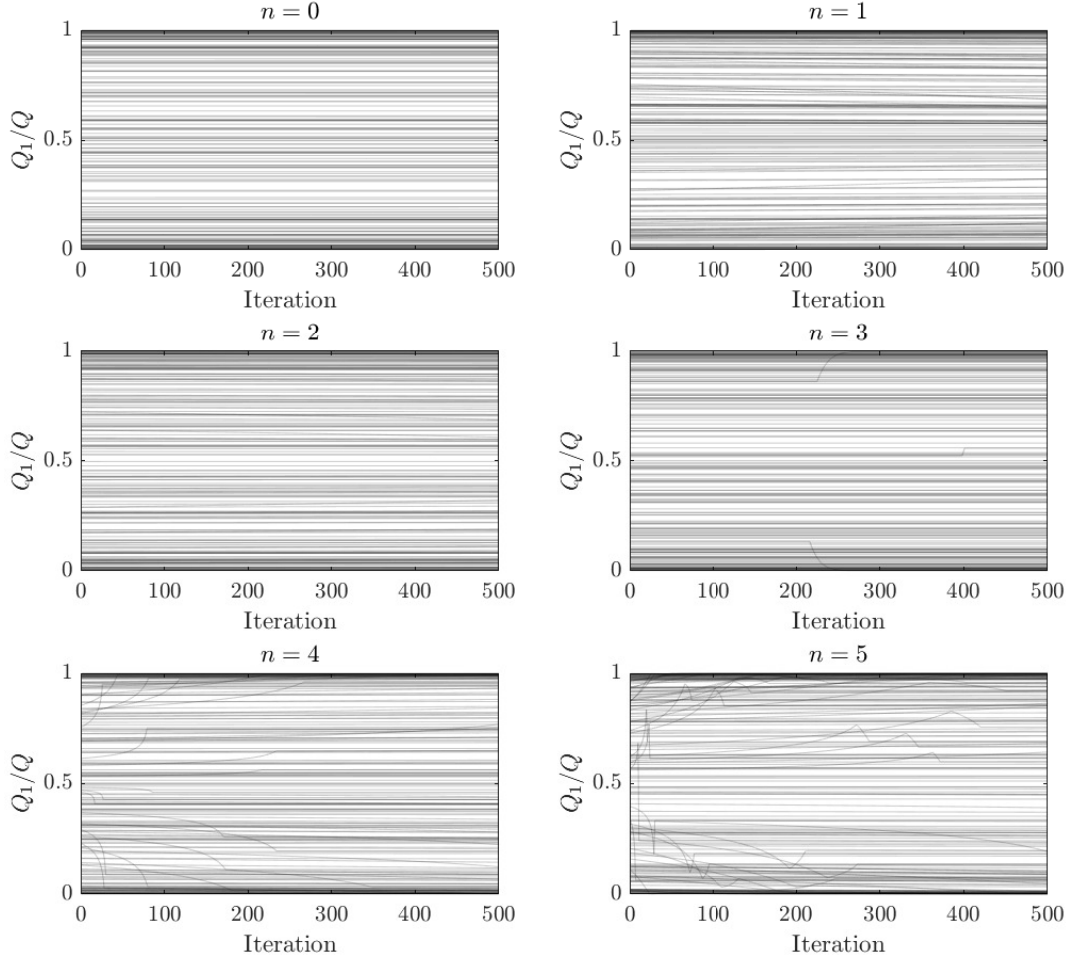

Figure 11: Two resistors parallel together

15

Figure 12: Toy model for two pipes in series. In each iteration, we change the radius of the pipe as $r_{\mathrm{new}} = r_{\mathrm{old}} - \alpha Q_i / r_{\mathrm{old}}^n$. Note that we set a maximum change of $\Delta r = \min 1, r$.

6 Permeability modification model

All the models introduced above represent different scenarios where the clogging/erosion might happen. The question, however remains that what could be a microscopic model? What it can predicts? and is there a proxy (bulk property) that can be observed to study the microscopic model?

We propose the following microscopic model: The polymers passing through pores are dragged by the flow. There are two forces competing when a polymer adheres to the surface of a pore (1) The drag force on the particle coming from flow, and (2) ionic/VanderWaals or whatever force that tries to adhere the particles to the surface. A particle attaches to the surface if the drag force exerted by the fluid flow around it is smaller than the VanderWaals/ionic force.

For simplicity, I assume that the force is ionic with a force distance profile of $F = K/X^2$, where K is a constant and X is the distance. I assume that polymers have an effective radius of d_p and fluid viscosity is μ and the flow rate is Q. This model states that the particle attaches to the surface when

$$F_{\text{drag}} \leq F_{\text{ionic}} \tag{83}$$

$$6\pi\mu d_p \frac{2Q}{\pi R^2}\left(1 - \frac{r^2}{R^2}\right) \leq \frac{K}{(R-r)^2} \tag{84}$$

$$1 - \frac{r^2}{R^2} \leq \left(\frac{K}{12\mu d_p Q}\right)\frac{1}{(1-r/R)^2} \tag{85}$$

$$1 \leq \frac{r^2}{R^2} + \alpha\frac{1}{(1-r/R)^2} \tag{86}$$

where $\alpha = K/\left(12\mu d_p Q\right)$ is a factor that compares the ionic force and viscous force. Note that it depends on the flux rate. If we define $x = 1 - r/R$ we obtain

$$1 \leq (1-x)^2 + \frac{\alpha}{x^2} \tag{87}$$

$$x^2 - x^2(1-x)^2 \leq \alpha \tag{88}$$

$$x^2(1 - (1-x)^2) \leq \alpha \tag{89}$$

$$x^3(2-x) \leq \alpha \tag{90}$$

$$\text{if } x \ll 1 \rightarrow x \leq \left(\frac{\alpha}{2}\right)^{1/3} \tag{91}$$
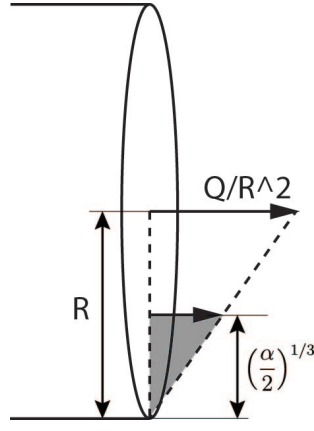
Figure 13: Flow in the pipe

As a result the distance is proportional to $\alpha^{1/3}$. Note that α depends on $1/Q$. Now, lets find the flux passing through this adsorption layer (any polymer in this layer would attach to the surface)

$$\text{volume/time} = \frac{1}{2}R\alpha^{1/3} \cdot \frac{Q}{R^3}R\alpha^{1/3} \cdot 2\pi R = \pi Q\alpha^{2/3} = \pi \left(\frac{K}{12\mu d_p}\right)^{2/3} Q^{1/3} \tag{92}$$

$$\text{volume/time} \propto Q^{1/3} \tag{93}$$

Now, if we assume that the number of polymers passing through the area cause clogging of the pipe and change the total area of the pipe, then we find that

$$d(\pi R^2) \propto Q^{1/3} \quad \rightarrow \quad RdR \propto Q^{1/3} \tag{94}$$

We also know that $k = \pi R^4/8l^2$, as a result

$$dk \propto R^3 dR \tag{95}$$

$$dk \propto R^2 Q^{1/3} \tag{96}$$

$$dk \propto Q^{1/3} \tag{97}$$

Experimental Results

In Shima's paper, we report a figure that shows the evolution of permeability k per volume of polymer V_{pol} that passes through the porous media. Basically we are plotting Δk versus Q passing through the porous media. The figure and best polynomial fit is shown blow
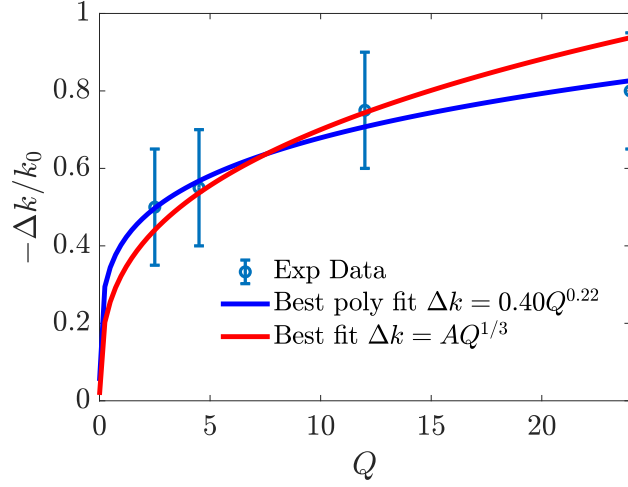
Figure 14: k versus volume of fluid passed through a porous media

7 Foam Relaxation and Non-monotonic Aging

So far the observation is that no matter how much disorder we introduce in the size distribution of pipe diameters, no relaxation behavior can be observed in a structured random network of tubes. If we prune the network, near the percolation limit, the slow $log(t)$ dynamics is observable, however, it seems to be very unlikely that it is the case. We need to introduce a toy model that can capture this behavior. My intuition is that the relaxation is due to aging of the adhesion of pore surfaces attaching to each other due to compression.

8 Flow-Chains: Force-Chains

We observe patterns similar to force-chains observed in granular materials, but in porous media. See Fig. 15. For a movie of this behavior see this link.
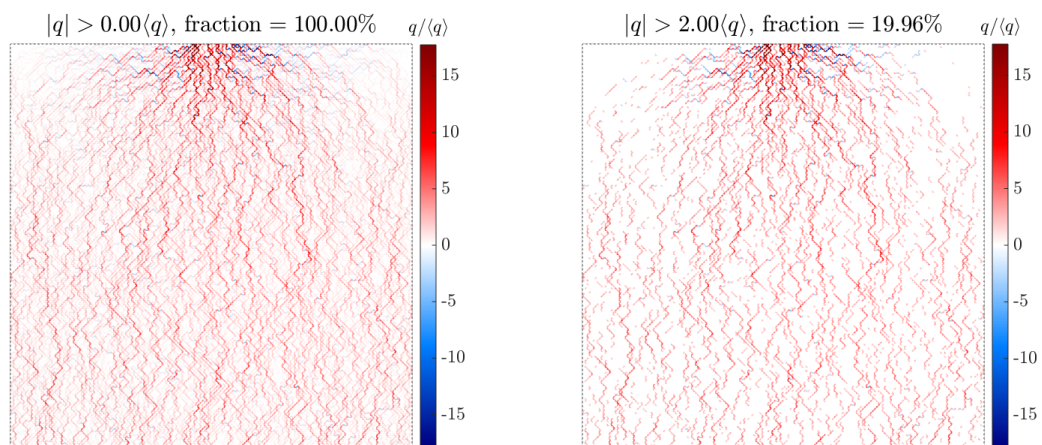
Figure 15: Force chain behavior in porous media.